Structural properties of a peptide derived from H+-V-ATPase subunit *a*

Louic S. Vermeer [a,b,c], Valérie Réat [a,b], Marcus A. Hemminga [c,*], Alain Milon [a,b,*]

[a] *Université de Toulouse, UPS; IPBS, 205 route de Narbonne, 31077 Toulouse Cedex, France*
[b] *CNRS, UMR 5089, Toulouse, France*
[c] *Laboratory of Biophysics, Dreijenlaan 3, 6703 HA Wageningen, The Netherlands*

ARTICLE INFO

ABSTRACT

The 3D structure of a peptide derived from the putative transmembrane segment 7 (TM7) of subunit *a* from H+-V-ATPase from *Saccharomyces cerevisiae* has been determined by solution state NMR in SDS. A stable helix is formed from L736 up to and including Q745, the lumenal half of the putative TM7. The helical region extends well beyond A738, as was previously suggested based on NMR studies of a similar peptide in DMSO. The pKa of both histidine residues that are important for proton transport was measured in water and in SDS. The differences that are found demonstrate that the histidine residues interact with the SDS polar heads. In detergent, circular dichroism data indicate that the secondary structure of the peptide depends on the pH and the type of detergent used. Using solid-state NMR, it is shown that the peptide is immobile in phospholipid bilayers, which means that it is probably not a single transmembrane helix in these samples. The environment is important for the structure of TM7, so in subunit *a* it is probably held in place by the other transmembrane helices of this subunit.

© 2009 Elsevier B.V. All rights reserved.

1. Introduction

Vacuolar H+-ATPase (V-ATPase) is an 830 kDa integral membrane protein responsible for the acidification of intracellular compartments. The pH of these cellular compartments plays an important role in many biological processes. The V-type ATPase protein has also been detected in the plasma membrane of specialised cells in various species, including humans. It is implicated in several diseases, such as osteoporosis and cancer. More detailed information can be found in reviews [1–7]. Much of the research has been carried out on V-ATPase from *Saccharomyces cerevisiae* (baker's yeast) and it has become a model for many eukaryotic V-ATPase studies.

V-ATPase consists of a cytoplasmic domain (V_1) and a transmembrane domain (V_0). Both domains contain several subunits. The V_0 transmembrane domain consists of subunits *a*, *c*, *c′*, *c″* and *d*. The current consensus is that proton translocation takes place at the interface of subunit *a* and the rotating (*c*, *c′*, *c″*) subunits. Mutation of arginine-735 in putative transmembrane helix 7 (TM7) of subunit *a* completely inhibits proton transport [8]. The histidine residues at positions 729 and 743 located in this helix have also been found to influence the proton pumping activity [4]. A single glutamic acid residue in each of the *c* subunits has been shown to be essential for proton translocation. Cysteine cross-linking studies suggest that TM7 from subunit *a* interacts with TM4 in subunits *c* and *c′* [9] and with TM2 in subunit *c″* [10]. By these effects, TM7 is likely to experience several important changes in its environment during proton translocation.

It has been shown that membrane-spanning peptides can be used as a model for their structure and dynamics in the entire protein [11–17]. A similar approach has recently been used to collect structural data on the transmembrane domain of subunit *e* from yeast F_1F_0-ATP-synthase [17]. Several studies on peptides derived from V-ATPase have been published. Different peptides derived from TM7 were studied by NMR in DMSO [18,19], by fluorescence in lipids [20], by ESR in SDS [22], by ESR and IR spectroscopy in lipid bilayers [23] and by CD and fluorescence in amphipols [24]. A high-resolution structure of the entire subunit *a* has not yet been elucidated, but a structure of a peptide called sMTM7 (see Table 1) derived from TM7 from subunit *a* was obtained by NMR studies in DMSO. A related peptide (MTM7, see Table 1) was studied in SDS, but gave NOESY spectra with severely broadened cross peaks [19].

For the present work, we decided to use a different peptide derived from TM7, called KMTM7 (see Table 1). Peptide KMTM7 contains two non-native lysine residues at the N and C terminal ends to try and improve its reconstitution in lipid bilayers. It also contains the essential arginine residue at position 735 as well as the two histidine residues at positions 729 and 743 from TM7 of V-ATPase subunit *a*. These residues are known to affect proton translocation. We used CD, liquid state NMR and solid state NMR spectroscopy of the peptide in different detergents and in the presence of lipid bilayers to assess its structural properties. A pH titration provided information about the effect of the protonation state of the histidine residues on the structure of the peptide.

2. Materials and methods

2.1. Peptide design and synthesis

Peptide KMTM7 (Table 1) was designed based on its putative localisation in the lumenal hemi-channel. Note that this is different from peptides that were designed earlier, because a recent paper on the topology of subunit *a* proposed that it consists of 8 transmembrane helices [25], in contrast to the now old model that assumed 9 transmembrane segments [2]. Nearly the entire putative membrane spanning region has been studied in DMSO, but a structure calculation was unsuccessful in both DMSO and SDS [19]. Given that peptide MTM7 is probably too long to span a membrane, peptide KMTM7 was designed to span the lumenal hemi-channel only, and is expected to have a length similar to a POPC/POPG membrane. To try and improve its reconstitution in lipid bilayers, two non-native lysine residues were added at the N- and C-termini. Throughout this paper the sequential numbering of amino acid residues of peptide KMTM7 is identical to the one used for subunit *a* in V-ATPase (Table 1). Peptide KMTM7 was produced on solid support using continuous flow chemistry by Pepceuticals Ltd., Leicester, UK. Its purity was tested by HPLC and mass-spectrometry and found to be greater than 90%. Peptide KMTM7 specifically labelled with ^{13}C on the carbonyl carbon of L734 was produced by Millegen biotechnology, Toulouse. Its purity was greater than 95%, as was demonstrated by HPLC and mass spectrometry. The carbonyl carbon of L734 was chosen as a labelling site because of its proximity to R735, the residue essential for proton translocation in V-ATPase.

2.2. Circular dichroism measurements

CD samples were prepared from a stock solution to make sure the concentration of peptide KMTM7 was equal in every sample (59 µM). For the CD studies in detergent, the SDS concentration was 82 mM and the octylglucoside concentration was 100 mM. The SDS concentration was chosen to be around 10 times the critical micelle concentration, 100 mM octylglucoside is about 3 times the CMC. Stock solutions of SDS and octylglucoside were prepared and adjusted with HCl or NaOH. After mixing the peptide with the stock solution, the pH was checked again. The final pH for each sample after having added the peptide is given in Fig. 1 in the Results section. CD spectra were recorded in the stepwise scanning mode from 190–350 nm on a Jasco J-815 CD spectrometer with a PTC-423S/15 temperature controller. The temperature was kept constant at 20 °C. A cuvette with a path length of 1 mm was used. The sensitivity was set to 100 mdeg, pitch was 0.5 nm, response was 1 s, and bandwidth was 2 nm. Two spectra were accumulated and averaged. Because of possible differences in the solubility of the peptide in the different detergents, the sample concentration was calculated by using the absorption at 280 nm and the theoretical extinction coefficient of the peptide [26], which was 6970 cm^{-1} mol^{-1}. CD spectra were corrected for the measured concentration and expressed in molar ellipticity (per residue) $[\theta]=\theta/(10\cdot C\cdot l\cdot n)$, where θ is the observed ellipticity in mdeg, C is the

Table 1
Amino acid sequence of the putative TM7 from yeast V-ATPase subunit *a*, and some of the peptides derived from it that have been studied.

	715	720	725	730	735	740	745	750	
Putative TM7	IHQVIHTIEFCLNCVSHTASYLRLWALSLAHAQLSSVLWT								[2]
MTM7	IHTIEFCLNCVSHTASYLRLWALSLAHAQLSSVLWTM								[19,22]
sMTM7	EFCLNCVSHTASYLRLWALSLAHAQ								[18,21]
KMTM7 (this study)	KKSHTASYLRLWALSLAHAQLSSKK								[20]

Note that when most of the previous peptide studies were carried out, the putative TM7 was different [2] from the currently (revised) topology of TM7 [24]. The peptide used in this study (KMTM7) runs from S728 to S748 and thus contains the residues in TM7 that have been shown to be important for proton transport. The current topological model places peptide KMTM7 in the lumenal side of the membrane, where it may be lining the lumenal hemi-channel. Two lysine residues were added at the N and C-termini to try and improve reconstitution in lipid bilayers. Throughout this paper, the numbering is the same as in the native protein.

molar concentration, l is the path length in cm and n is the number of residues.

2.3. Solid state NMR spectroscopy

For solid-state NMR, peptide KMTM7 was specifically labelled with ^{13}C on the carbonyl carbon atom of L734. Peptide KMTM7 (2.3 mg) was mixed with 25.2 mg POPC and 6.3 mg POPG in 2 ml methanol, which led to a POPC/POPG ratio of 80/20 (mol/mol) and a peptide/lipid ratio of 1/50. The sample was shaken continuously overnight, under nitrogen atmosphere at room temperature. The methanol was evaporated off and the sample was placed under vacuum to remove any residual solvent. The dry sample was re-hydrated with 500 µl, 10 mM sodium phosphate buffer at pH 7.1 and centrifuged at 12,100 *g* for 10 min to precipitate the proteoliposomes. The pellet was put in a 3.2 mm magic angle spinning rotor and extra water was added to obtain full hydration (about 30 water molecules per lipid, as determined by weighing the sample). The sample was homogenised by centrifugating 8 times (3000 *g*, 1 min), while turning the sample over after each centrifugation. ^{13}C solid-state NMR spectra were recorded the same day on a Bruker Avance 700 MHz spectrometer equipped with a 3.2 mm magic angle spinning triple resonance probe. A standard cross-polarisation pulse sequence was used, with a cross polarisation spin lock field of 40 kHz and a contact time of 1.4 ms. A TPPM proton decoupling pulse sequence was applied during the acquisition time, with a 58 kHz decoupling field. The relaxation delay was set to 2 s. ^{13}C MAS spectra of the labelled L734 residue (Fig. 2) were recorded at a spinning frequency of 4 kHz. The temperature was kept constant at 302 °K, which is well above the main gel to liquid crystalline phase transition temperature of the lipid mixture. For comparison, spectra of dry peptide powder were acquired as well. Before Fourier transformation, a Lorentzian line broadening of 50 Hz was applied. Spectra were referenced to DSS and the standard conventions were used in the analysis of the chemical shift anisotropy. The intensities of the observed spinning sidebands were subjected to a Herzfeld–Berger analysis [27] using the DMFIT software [28] to extract the anisotropy (δ_{CS}) and asymmetry (η) parameters of the chemical shift tensor.

2.4. Histidine titration by liquid state NMR spectroscopy

Samples for the pH titration by liquid state NMR were prepared by adding 1 ml of either D$_2$O or SDS solution to 2 mg of peptide KMTM7, giving a peptide concentration of 718 µM. The SDS concentration was chosen to give a 1/250 peptide/detergent molar ratio in all the NMR experiments. In the CD experiments, this ratio had to be higher in order to be well above the CMC. After vortexing, the samples were centrifuged for 10 min at 12,100 *g* to remove any precipitated peptide. The supernatant was transferred to a different tube, and the pH was
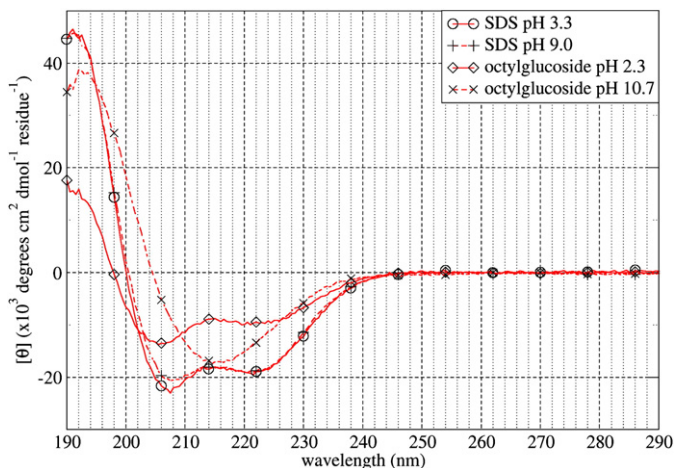
Fig. 1. Circular dichroism. Circular dichroism spectra of peptide KMTM7 in SDS and in octylglucoside at a pH above and below the histidine pKa.

Fig. 2. Solid state NMR. Top: 4 kHz CPMAS ^{13}C NMR spectrum of the ^{13}C labelled carbonyl carbon of the L734 residue in peptide KMTM7 in the presence of hydrated POPC/POPG bilayers. The isotropic peak at 174.5 ppm is marked with a star. The sharp peaks at 176.0 and 132.2 ppm are assigned to the ^{13}C natural abundance in the carbonyl carbon of the lipids and the double bond in the lipid tails, respectively. Bottom: 4 kHz CPMAS ^{13}C NMR spectrum of dry peptide powder (without lipids), for comparison.

adjusted with DCl stock solution. DSS was added (30 µl, 5 mM) as standard to calibrate the spectra. Before recording an NMR spectrum, the pH was increased stepwise for each consecutive data point by adding the required amount of a 100 mM NaOD solution. ^{1}H NMR spectra were recorded on a Bruker Avance 600 MHz spectrometer with a 5 mm TCI cryoprobe. The sample temperature was kept constant at 298 °K. The rf-field for the [1]H 90° pulse was 21 kHz. The relaxation delay was 1 s and the signal from residual water was suppressed by pre-saturating the water protons with a 31 Hz continuous wave pulse during this delay. For each data point, 512 scans were accumulated. To calculate the pKa value from the experimental data, the GOSA computer program [29] was used to at the data points to the following equation $CS_{observed} = (CS_1 + CS_2 \cdot 10^{(pH - pKa)}) / (1 + 10^{(pH - pKa)})$. In this equation CS_1 and CS_2 are the chemical shift of the protonated and deprotonated state of the histidine residue. Fitting of three parameters (CS_1, CS_2 and pKa) resulted in a determination of the pKa values.

2.5. NMR structure determination

For the structure determination, ^{1}H NMR experiments were carried out. The peptide KMTM7 (1.8 mg) was dissolved in 1 ml of TFE. SDS-d25 was dissolved in 10 mM NaH_2PO_4 buffer (pH 3.0) to get a 160 µM solution, which was added to the peptide solution. After 5 min, 15 ml water was added and the sample was left under argon gas on a shaking table at room temperature overnight. The next day, the sample was frozen in liquid nitrogen and freeze-dried. The resulting white powder was dissolved in 636 µl buffer (10 mM NaH_2PO_4, pH 3.0, 10% D_2O), giving a final concentration of 1 mM peptide in 250 mM SDS. Because a white precipitate was visible, the sample was centrifuged at 21,100 g for 2 min. The supernatant was transferred to an NMR tube and DSS was added (final concentration 0.3 mM) to calibrate the NMR spectra. The final pH of the sample was 5.0. The NMR tube was filled with argon gas and closed with a plastic cap and parafilm. NMR spectra indicated that the sample was stable for at least 2 months (no changes in the 1D and 2D ^{1}H spectra), when stored at room temperature. NOESY and TOCSY spectra were recorded on a Bruker Avance 600 MHz spectrometer with a 5 mm TCI cryoprobe. The sample temperature was kept constant at 298 °K or 313 °K (two sets of experiments). The mixing time was 80 ms for the TOCSY spectra and 300 ms for the NOESY spectra. The spectral width was 12 ppm and the [1]H 90° pulse length was 12.5 µs. A WATERGATE pulse sequence was used to suppress the water signal. The data processing was done with Bruker Topspin software (version 1.3). The free induction decay was multiplied by a shifted-sine[2] window function. The line broadening was set to 10 Hz and a forward linear prediction was applied. After
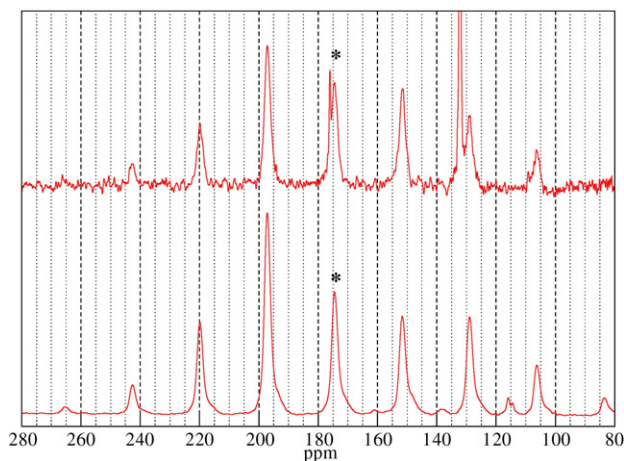
Fourier transformation, the spectra were phase corrected and a baseline correction was applied. The NMR spectra were calibrated using the DSS signal at 0 ppm. Peak picking and integration were done using the software package Sparky 3.113 [30]. The calculation of the CSI and NOE contact tables were carried out using a Perl script that read a Sparky peak list as input file. Four different reference sets for the H_α random coil chemical shifts were tested and all led to approximately the same result. Results presented in this paper used the reference set from [31].

The structure calculation was carried out using ARIA 2.2 software [32] with CNS 1.2 [33]. Only fully assigned NOEs were used in the structure calculation. No dihedral angle restraints were imposed. The default ARIA settings were used, but the number of trial structures was increased to 100 for each iteration step, of which the best 20 structures were used as input for the subsequent iteration. This led to a better convergence in the final 20 structures. No spin diffusion correction was applied during the calibration steps, because a structure calculation with corrections for spin diffusion resulted in structures that were similar to those without the correction. The
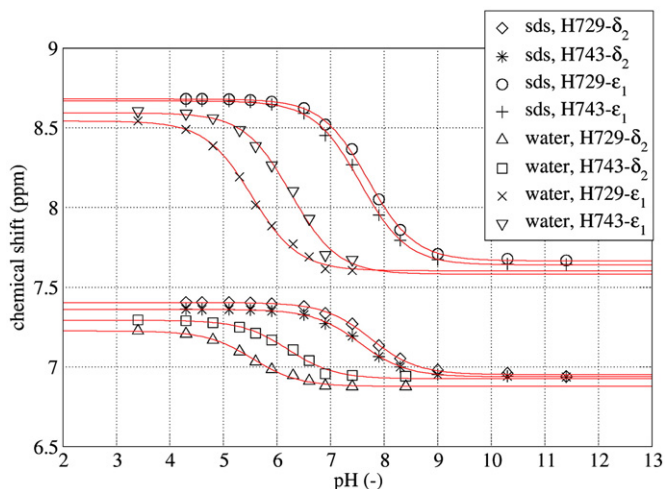

Fig. 3. His titration and pKa determination. Titration curves of H729 and H743 of peptide KMTM7 in 180 mM SDS and in water, at 298 °K. The symbols are experimental data points; the curves are the best fit to the data, used to calculate the pKa values.
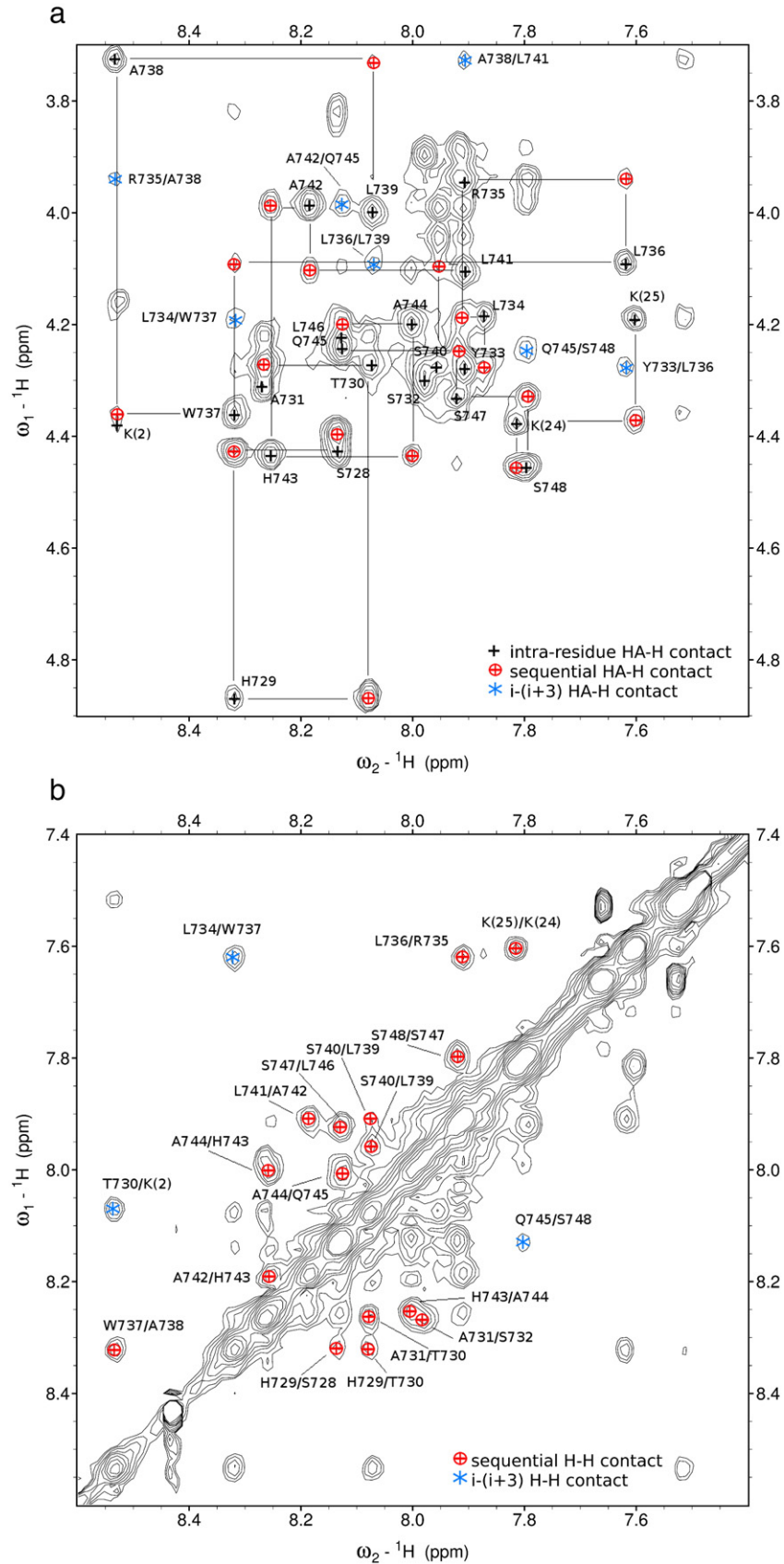
Fig. 4. (a) KMTM7 in SDS, NOESY spectrum. The H_N–H_α fingerprint region of the NOESY spectrum of peptide KMTM7 in SDS at pH 5.0, 313 °K, recorded at 600 MHz with a mixing time of 300 ms. Intra-residue contacts are labelled with black crosses, sequential HA–H contacts are shown as (red) crosses in circles and $i-(i+3)$ contacts are labelled with (blue) stars. Other contacts are not labelled for presentation reasons, but all peaks that are visible in the figure were assigned. (b) The H_N–H_N fingerprint region of the same spectrum. Sequential H–H contacts are labelled with (red) crosses in circles and $i-(i+3)$ contacts are labelled with (blue) stars.

	K	K	S	H	T	A	S	Y	L	R	L	W	A	L	S	L	A	H	A	Q	L	S	S	K	K
Hα-HN																									
Hβ-HN																									
HN-HN																									
Hα-Hβ																									
Hα-HN																									
HN-HN																									

Fig. 5. Inter-residue NOE connectivities. Some of the inter-residue NOE connectivities. Only contacts that were kept (by ARIA) for the calculation of the final structure are shown. The first three rows show $i-(i+1)$ contacts, the bottom three rows are $i-(i+3)$ contacts. A list of the contacts that were used in the final structure calculation can be found in the BMRB database under number 11056.

manually assigned NOE's were defined as "trusted", meaning that ARIA was not allowed to change the assignments. After the last iteration, a final refinement step was carried out in water. The PROCHECK-NMR software [34] and a Perl script were used to check the quality of the structures.

3. Results

3.1. Peptide conformation depends on environment

The CD experiments (Fig. 1) indicate that the α-helical content of peptide KMTM7 strongly depends on the pH and the detergent used. Note that "helical content" may have two different interpretations: either the structure of each molecule in the ensemble is less helical, or a part of the molecules are helical while another population contributes to the CD spectrum with a different conformation (such as for instance SDS-bound and unbound molecules). In SDS, the line shape of the CD spectra indicated a helical content around 60% for an α-helix both at pH 3.3 and 9.0 (below and above the histidine pKa), in agreement with the NMR data. The intensity of both spectra was the same. Analysis with the CDPro [35] software reports 62% and 59% of helix, respectively, and the various deconvolution algorithms within CDPro (selcon3, cdsstr and continll) gave consistent results. In octylglucoside an α-helix is observed at pH 2.3, while at pH 10.7 a β-sheet is found. The low signal intensity in octylglucoside at pH 2.3 indicates that the α-helical content is lower than in SDS. The fitting software reports 34% helix at pH 2.3 and 43% helix at pH 10.7, a result which does not seem to agree with the line shape of these spectra (see discussion of the Results). An α-helical line shape with two minima at 207 and 222 nm was also observed in samples at pH 4, while at pH 5 the spectrum had only one minimum at 216 nm, typical for a β-sheet (data not shown).

The CPMAS NMR spectrum of the ^{13}C labelled carbonyl carbon of the L734 amino acid residue in peptide KMTM7 in the presence of hydrated POPC/POPG bilayers is shown in Fig. 2 (top). We do not believe that the peptide is reconstituted as a transmembrane α-helix, as will be discussed in the Discussion section of this paper. The sharp peaks at 176.0 and 132.2 ppm are assigned to the ^{13}C natural abundance in the carbonyl carbon of the lipids and the double bond in the lipid tails, respectively. Fig. 2 (bottom) shows the CPMAS ^{13}C NMR spectrum of dry peptide powder (without lipids). For the dry peptide powder, the anisotropy $\delta_{CS} = -84$ ppm and the asymmetry parameter $\eta = 0.60$. In the hydrated lipid bilayers, $\delta_{CS} = -77$ ppm and $\eta = 0.75$.

3.2. The pKa of the histidine residues

To determine the pKa of the histidine residues of peptide KMTM7, the chemical shift of its protons was followed during a pH titration [36]. It is not possible to measure the titrated δ_1 and ε_2 amine protons directly, because they exchange with the deuterons from the solvent. Therefore, a titration curve was measured by following the changes in ^{1}H chemical shift of the δ_2 and ε_1 protons. Their chemical shift changes because the shielding increases when the neighbouring nitrogen atom is deprotonated. The signal from the four protons of the two histidine residues was assigned based on the two characteristic singlets around the expected chemical shift values. This assignment was confirmed by monitoring the change of the peak positions when the pH was raised. In Fig. 3 the titration curves of H729 and H743 are shown. In SDS, the curve with the pKa that is slightly higher is assigned to H729 and the lower pKa curves to H743 (using the NOESY spectra). The pKa values in SDS are 7.7 and 7.6. In water one histidine residue has a pKa of 6.3 and the other residue has a pKa of 5.5. It is likely that the residue with a pKa of 5.5 is H729, because the proximity
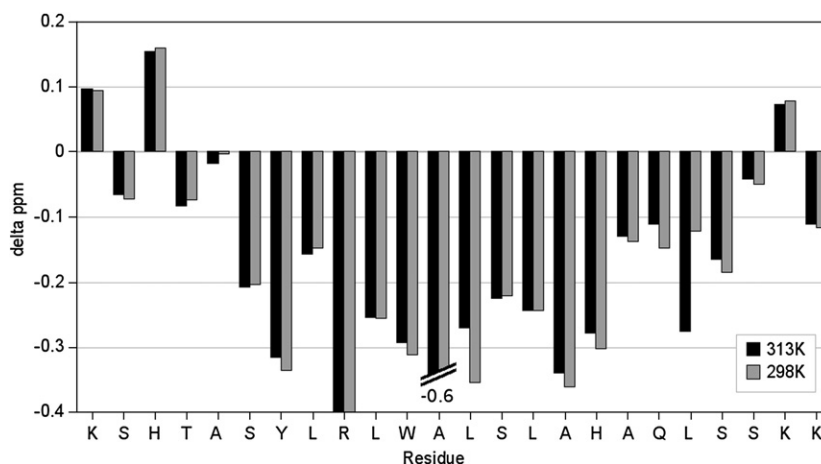

Fig. 6. Chemical shift index. Chemical shift differences between the H$_\alpha$ chemical shift in the peptide and reference values for a random coil [30].

of the two positively charged lysine residues probably destabilises the protonated state. The residue with a pKa of 6.3 would then be H743. A titration in octylglucoside was not successful, because the peptide precipitated above pH 5 leading to a loss of NMR signal. The CD results in octylglucoside agree with this observation.

3.3. Structure of the peptide KMTM7 in SDS

3.3.1. Analysis of the assignments

The H_α–H_N fingerprint region of the NOESY spectrum at 313 °K is shown in Fig. 4a and the H_N–H_N region in Fig. 4b. Except for the first lysine residue, all of the residues could be (at least partly) assigned in the spectra at 313 °K and 298 °K (not shown). In Fig. 5 an overview of some 7 of the inter-residue contacts is shown. Sequential cross-peaks were found for nearly all residues. An almost continuous stretch of $i−(i+3)$ contacts is observed between Y733 and Q745 at 313 °K: a clear indication of a helical structure in that region. Although these contacts are not observed in all regions of the peptide, other typical contacts for a helix are visible. Only one long range contact $(i−i+4)$ was observed. Most of the contacts that were present at 313 °K could also be found in the spectrum at 298 °K. Several contacts could be assigned in only one of the spectra. This is probably due to overlapping cross-peaks because many resonances had slightly shifted after the temperature change.
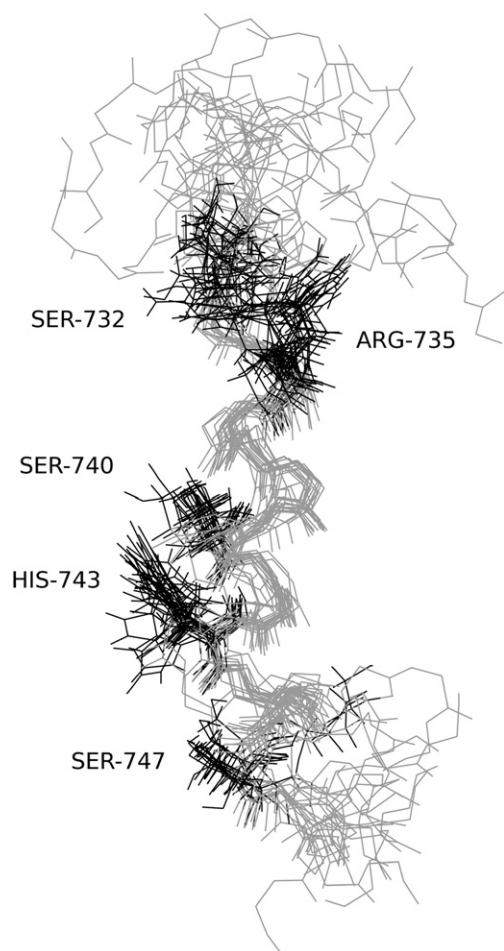

Fig. 7. Structure of KMTM7 in SDS. Structure of peptide KMTM7 in SDS after refinement. A superposition of the 20 best structures is shown. The structures were aligned by pairwise fitting of the backbone atoms of residue 623 to the mean molecule, using the software package MOLMOL [38]. The RMSD of the fit was 1.7 Å (calculated on backbone atoms from residues 6–23). The trace of the backbone is shown as a thin grey line. The side chains of the polar residues in the structured region of the peptide are shown in black. The structures were deposited in the RCSB protein data bank with reference number 2rpw.

Table 2a
The quality of the 20 best structures before and after refinement.

Refinement	No	Water
Favored	52%	58%
Allowed	35%	34%
Generously allowed	13%	7%
Disallowed	1%	2%

Percentages correspond to the number of dihedral angles that fall in the different regions of a Ramachandran plot.

The chemical shift of the H_α protons strongly depends on the secondary structure of a protein or peptide. An up-field shift with respect to a random coil structure (a negative CSI value) indicates an α-helical region, while a downfield shift is indicative of β-sheets [37]. A difference that is more negative than −0.1 for 3–4 consecutive residues is usually considered an alpha helical region. Fig. 6 shows the H_α chemical shift difference from a reference set with random-coil chemical shifts.

3.3.2. Structure calculation

The structure calculation was carried out using a combination of both the spectra recorded at 298 °K and 313 °K. A superposition of the 20 best structures after minimization in water is shown in Fig. 7. The high convergence of these structures indicates an accurate and well defined structure. The average RMSD of the backbone atoms to the mean molecule was 1.7 Å, calculated from residues 6–23. Other quality checks (Table 2a) and the number of NOEs used (Table 2b) confirm the quality of the result. The structures were deposed in the RCSB protein data bank under number 2rpw. The side chain dihedral angles of H729 have largely different values in different structures, while R735 and H743 seem to be in a more defined conformation. Multiple side chain NOE contacts were assigned for these residues and very similar side chain dihedral angles were found before and after refinement, indicating that they are not an artefact of the refinement. The N-terminus up to residue A731 shows a broad distribution of backbone dihedral angles. A similar effect is observed for residue S748 up to the C-terminus. This is not unexpected, because peptides usually show a certain amount of flexibility on the termini. From Y733–S747, most residues have small deviations from the average angle, and the average values are close to those of an ideal α-helix with $\varphi = −57.8$ and $\psi = −47.0$. The dihedral angles are consistent with the CSI data (Fig. 6). Fig. 8 shows an analysis of the secondary structure using the extended Kabsch and Sander method [39], as carried out by the PROCHECK NMR software [34]. An α-helix is assigned from L736 to L741 in most structures. The regions around the α-helical middle of the peptide tend to exhibit 3_{10} helical structures or hydrogen bonded turns. Although the N-terminus of the peptide seems rather flexible, it appears to be capable of forming helices, given the large number of structures that form hydrogen bonded turns in this region of the molecule.

4. Discussion

The structural properties of a peptide derived from V-ATPase subunit *a* TM7 were studied. The peptide is different from the ones used in previous structural studies [18,19], but it also contains the R735 residue that is essential for proton transport. In addition, two lysine residues were added to each of the termini. NMR experiments in a membrane-mimicking environment gave better spectra than in previous studies, allowing a structure determination in SDS. Furthermore, the use of SDS instead of DMSO (that was used previously [18,19]) allowed us to control the pH of the sample. NMR experiments enabled us to study the structure around residue R735 in detail, while CD studies in SDS and octylglucoside provided information on how the structure of the peptide is influenced by its environment. The role

Table 2b
Number of NOEs used for the structure calculation after the final iteration.

Total	Intra-residue	Inter-residue	$i-(i+1)$	$i-(i+2)$	$i-(i+3)$	$i-(i+n)$ $n>3$	Short ≤ 2.5 Å	Medium ≤ 3.5 Å	Long >3.5 Å	Violations[a]
270	141	129	83	10	35	1	177	82	11	5.7

[a] Average number of violated NOEs in the 20 lowest energy structures.

that the histidine residues play in these structural changes was investigated by determining the protonation state (pKa) of the histidine residues in SDS and in water.

The CD experiments shown in Fig. 1 indicate that the structure of the peptide KMTM7 depends on the pH and on its environment. An α-helical structure is observed in SDS, regardless of the pH. In octylglucoside, the peptide loses its α-helical structure at high pH in favor of a β-sheet conformation, indicating aggregation. The aggregation in octylglucoside is ultimately visible as a white precipitate in the sample. Possibly, the charged histidine residues prevent the peptides from aggregating at a low pH. When uncharged, the peptides interact and aggregate to β-sheets. In SDS, the negatively charged surface of the micelles may prevent the peptides from coming close enough to interact and aggregate, even at high pH. The difference in intensity that is observed between the CD spectra in octylglucoside and SDS may be due to a lower helical content, but uncertainties in the concentration prevent an accurate determination of the helical content. It is well known that the percentage of helicity calculated from CD spectra is often inaccurate, and very sensitive to the accuracy in the sample concentrations. The percentages of helix in SDS agree with the NMR results, but based on the line shape of the spectra the calculation of the percentage of helix in octylglucoside seems inaccurate, which is probably a result of inaccuracies in the sample concentration due to precipitation and the formation of micro-aggregates of peptides.

Solid-state NMR measurements of peptide KMTM7 in the presence of lipid vesicles indicated that it is more mobile in the presence of lipid membranes than as a dry powder ($|\delta_{CS,lipids}| < |\delta_{CS,powder}|$), and its asymmetry ($\eta = 0.75$) does not correspond to the expected asymmetry of a single transmembrane α-helix with a fast axial diffusion around the bilayer normal (which would have given $\eta = 0$). From this information we conclude that we did not succeed to reconstitute the peptide as a transmembrane helix in lipid bilayers. Several lipid mixtures and different reconstitution protocols have been tried, all with the same, negative, result. We conclude that this peptide does not behave like a typical transmembrane peptide, as is illustrated by

Fig. 8. DSSP secondary structure assignment. DSSP code (Kabsch and Sander) secondary structure assignment of the twenty minimized structures shown in Fig. 7. The structure assignment was carried out with procheck_nmr. Capital letters are the original Kabsch and Sander definitions, non-capitalized letters indicate the slightly extended assignment that is used by procheck. H/h = α-helix, G/g = 3₁₀-helix, I/i = π-helix, T/t = hydrogen bonded turn, S = bend.

the solid state NMR spectrum in Fig. 2. Furthermore, the ^{13}C isotropic chemical shift of L743 is not typical for an α-helical conformation. These solid-state NMR results in the presence of phospholipid bilayers do not fit with the previously shown α-helical transmembrane conformation from fluorescence data [20]. This may be due to the high concentration and low hydration required for these MAS NMR experiments. Since in similar experimental conditions, typical α-helical behaviour has been observed for other peptides, we can conclude that peptide KMTM7 has a strong tendency of structural polymorphism, as has already been observed by circular dichroism.

Depending on the environment, the pKa of the two histidine residues changes markedly (Fig. 3). Obviously, the pKa that was measured in our samples cannot be directly compared to the pKa in the native environment of the peptide. Especially the artificial lysine residues near H729 are expected to influence its pKa. However, the environmentally induced pKa differences in peptide KMTM7 help to explain the complex behaviour of the peptide in the different detergents. For the structure determination by 2D NMR experiments, it also allowed us to choose a pH where the protonation state of the histidine residues is known. The difference in pKa between the sample in water and in SDS is higher for H729 than for H743. The protonated state of H729 is destabilised in water, probably due to the presence of the non-native lysine residues. In SDS it has almost the same pKa as H743, because both are surrounded by negatively charged SDS headgroups. Therefore, these data clearly indicate that both histidine residues interact with the SDS headgroups. They are not located in a hydrophobic environment inside a micelle, which would have destabilised the charged state, and given a lower pKa in SDS. It has been previously demonstrated that charged histidine residues preferably interact with the negatively charged headgroup region, while uncharged histidine residues may take up a location in a hydrophobic environment [21].

Using peptide KMTM7 instead of MTM7 or sMTM7 greatly improved the quality of the NMR spectra in SDS (Fig. 4a,b), which allowed us to determine the structure in this detergent. The lysine, histidine and arginine residues were all charged under the experimental conditions used for the 2D NMR experiments. The N-terminus of the peptide shows more difference in the conformation of the 20 best structures (Figs. 7 and 8) than the C-terminus, which can be interpreted as more structural flexibility. In general, the C-terminus of peptides tends to be more flexible than the N-terminus [40], but this peptide shows more flexibility in its N-terminus, which we interpret as an effect of the primary structure. The charged lysine residues probably interact with the negative charges that are present in the interface region, which gives us an idea of the location of the SDS headgroups. This is in agreement with the results of the pKa measurement in SDS. The R735 side chain points towards the N-terminus of the peptide, presumably also to the interface region. This behaviour is common for arginine residues, and has previously been suggested in the case of the KMTM7 peptide in phospholipids bilayers [20]. The end of the R735 side chain is nearly located on the same side of the helix as H743 (Fig. 7). Although a helical wheel plot (not shown) does not clearly indicate a hydrophilic side of KTMT7 that could line the lumenal hemi-channel of V-ATPase subunit a, the fact that the arginine side chain is long enough to move to the same side of the helix as H743 may indicate that it is accessible through a hemi-channel that is lined by the residues on that side of the helix (R735–S740–H743–S747).

Peptide KMTM7 shows a helical structure in SDS from L736 up to and including Q745 (Fig. 8). The region around the α-helical core also

displays helical characteristics. In most of the structures, hydrogen-bonded turns are observed from S728 up to the N-terminus. The CSI values (Fig. 6) and CD spectra (Fig. 1) indicate a predominantly α-helical structure and are therefore consistent with the NMR structural data. Only one long-range $(i-(i+4))$ contact was observed (between the tyrosine HA and the HD1 proton from the tryptophan side chain), indicating that the peptide does not aggregate or fold back on itself in a hairpin or coil structure. In previous studies of MTM7 in DMSO, three helical regions were identified [19], spanning C723–A731, Y733–L739 and A742–V749, and it was suggested that TM7 is a 32 residue helical segment spanning from T719 to W751. Shortly afterwards, also in DMSO, two helical regions were identified more precisely in peptide sMTM7: C726–H729 and S732–A738 [18]. The current results suggest that the helical region can run at least up to S748, and that TM7 can form more a stable and better defined helical structure than previous results in DMSO suggest. A similar observation has been made for a peptide derived from F_1–F_0-ATPase [17]. A combination of the new and old experimental data indicates that TM7 can form helices consisting of mainly hydrophobic residues in a region that is much longer than is needed to span a biological membrane. This strongly suggests that TM7 interacts with other helices that are also longer than needed to span the membrane, which would shield the hydrophobic TM7 residues from the water phase. It may prove hard to accurately predict the transmembrane region of proteins with these properties using the common methods based on solvent accessibility and hydrophobicity scales. The data presented in this paper show that the helix may even extend up to S748. We do not believe that the non-native lysine residues that were added to the termini have greatly influenced the structure of the peptide. Firstly, the tendency to form helices was also demonstrated in DMSO for a similar peptide without lysine residues, and secondly, we do not know of any examples from the literature where the addition of charged residues to the termini forces the entire peptide to adopt a certain structure. All available data indicate that peptide KMTM7 is capable of helix formation, but is not the archetype of a helical transmembrane peptide in lipids as compared to WALP [41]. Therefore we conclude that peptide KMTM7 probably requires its native environment, consisting of subunits a and c to be held in place in the native protein. The recent suggestion that transmembrane helix 7 consists of almost 40 amino acids [25] corresponds well with this picture.

Acknowledgements

Appendix A. Supplementary data

Supplementary data associated with this article can be found, in the online version, at doi:10.1016/j.bbamem.2009.02.015.

References

[1] M.E. Finbow, M.A. Harrison, The vacuolar H+-ATPase: a universal proton pump of eukaryotes, Biochem. J. 324 (1997) 697–712.

[2] T. Nishi, M. Forgac, The vacuolar (H+)-ATPases—nature's most versatile proton pumps, Nat. Rev., Mol. Cell Biol. 3 (2002) 94–103.

[3] Y. Arata, T. Nishi, S. Kawasaki-Nishi, E. Shao, S. Wilkens, M. Forgac, Structure, subunit function and regulation of the coated vesicle and yeast vacuolar (H+)-ATPases, Biochim. Biophys. Acta 1555 (2002) 71–74.

[4] S. Kawasaki-Nishi, T. Nishi, M. Forgac, Proton translocation driven by ATP hydrolysis in V-ATPases, FEBS Lett. 545 (2003) 76–85.

[5] K.W. Beyenbach, H. Wieczorek, The V-type H+ ATPase: molecular structure and function, physiological roles and regulation, J. Exp. Biol. 209 (2006) 577–589.

[6] P.M. Kane, The where, when, and how of organelle acidification by the yeast vacuolar H+-ATPase, Microbiol. Mol. Biol. Rev. 70 (2006) 177–191.

[7] K.C. Jefferies, D.J. Cipriano, M. Forgac, Function, structure and regulation of the vacuolar (H+)-ATPases, Arch. Biochem. Biophys. 476 (2008) 33–42.

[8] S. Kawasaki-Nishi, T. Nishi, M. Forgac, Arg-735 of the 100-kDa subunit a of the yeast V-ATPase is essential for proton translocation, Proc. Natl. Acad. Sci. U. S. A. 98 (2001) 12397–12402.

[9] S. Kawasaki-Nishi, T. Nishi, M. Forgac, Interacting helical surfaces of the transmembrane segments of subunits a and c′ of the yeast V-ATPase defined by disulfide-mediated cross-linking, J. Biol. Chem. 278 (2003) 41908–41913.

[10] Y. Wang, T. Inoue, M. Forgac, TM2 but not TM4 of subunit c″ interacts with TM7 of subunit a of the yeast V-ATPase as defined by disulfide-mediated crosslinking, J. Biol. Chem. 279 (2004) 44628–44638.

[11] M. Katragadda, J.L. Alderfer, P.L. Yeagle, Assembly of a polytopic membrane protein structure from the solution structure of overlapping peptide fragments of bacteriorhodopsin, Biophys. J. 81 (2001) 1029–1036.

[12] S. Soulié, J.-M. Neumann, C. Berthomieu, J.V. Møller, M. le Maire, V. Forge, NMR conformational study of the sixth transmembrane segment of sacroplasmic reticulum Ca^{2+}-ATPase, Biochemistry 38 (1999) 5813–5821.

[13] F. Li, H. Li, L. Hu, M. Kwan, G. Chen, Q.-Y. He, H. Sun, Structure, assembly, and topology of the G185R mutant of the fourth transmembrane domain of divalent metal transporter, JACS 127 (2005) 1414–1423.

[14] V.Y. Orekhov, K.V. Pervushin, A.S. Arseniev, Backbone dynamics of (1–71) bacterioopsin studied by two-dimensional ^{1}H–^{15}N NMR spectroscopy, Eur. J. Biochem. 219 (1994) 887–896.

[15] P.L. Yeagle, A.D. Albert, Use of nuclear magnetic resonance to study the three-dimensional structure of rhodopsin, Methods Enzymol. 343 (2002) 223–231.

[16] F.-X. Ding, H. Xie, B. Arshava, J.M. Becker, F. Naider, ATR-FTIR study of the structure and orientation of transmembrane domains of the Saccharomyces cerevisiae α-mating factor receptor in phospholipids, Biochemistry 40 (2001) 8945–8954.

[17] H. Yao, R.A. Stuart, S. Cai, D.S. Sem, Structural characterization of the transmembrane domain from subunit e of yeast F_1F_0-ATP synthase: a helical GXXXG motif located just under the micelle surface, Biochemistry 47 (2008) 1910–1917.

[18] A.M. Duarte, E.R. de Jong, R. Wechselberger, C.P. van Mierlo, M.A. Hemminga, Segment TM7 from the cytoplasmic hemi-channel from V_0–H+ V-ATPase includes a flexible region that has a potential role in proton translocation, Biochim. Biophys. Acta 1768 (2007) 2263–2270.

[19] A.M. Duarte, C.J. Wolfs, N.A. van Nuland, M.A. Harrison, J.B. Findlay, C.P. van Mierlo, M.A. Hemminga, Structure and localization of an essential transmembrane segment of the proton translocation channel of yeast H+-V-ATPase, Biochim. Biophys. Acta 1768 (2007) 218–227.

[20] R.W. Hesselink, R.B. Koehorst, P.V. Nazarov, M.A. Hemminga, Membrane bound peptides mimicking transmembrane Vph1p helix 7 of yeast V-ATPase: a spectroscopic and polarity mismatch study, Biochim. Biophys. Acta 1716 (2005) 137–145.

[21] B. Bechinger, Towards membrane protein design: pH-sensitive topology of histidine-containing polypeptides, J. Mol. Biol. 263 (1996) 768–775.

[22] W.L. Vos, L.S. Vermeer, M.A. Hemminga, Conformation of a peptide encompassing the proton translocation channel of vacuolar H+-ATPase, Biophys. J. 92 (2007) 138–146.

[23] Z. Kóta, T. Páli, N. Dixon, T.P. Kee, M.A. Harrison, J.B.C. Findlay, M.E. Finbow, D. Marsh, Incorporation of transmembrane peptides from the vacuolar H+-ATPase in phospholipid membranes: spin-label electron paramagnetic resonance and polarized infrared spectroscopy, Biochemistry 47 (2008) 3937–3949.

[24] A.M. Duarte, C.J. Wolfs, R.B. Koehorst, J.-L. Popot, M.A. Hemminga, Solubilization of V-ATPase transmembrane peptides by amphipol A8-35, J. Pept. Sci. 14 (2008) 389–393.

[25] Y. Wang, M. Toei, M. Forgac, Analysis of the membrane topology of transmembrane segments in the c-terminal hydrophobic domain of the yeast vacuolar ATPase subunit a (vph1p) by chemical modification, J. Biol. Chem. 283 (2008) 20696–20702.

[26] S.C. Gill, P.H. von Hippel, Calculation of protein extinction coefficients from amino acid sequence data, Anal. Biochem. 182 (1989) 319–326.

[27] J. Herzfeld, A.E. Berger, Sideband intensities in NMR spectra of samples spinning at the magic angle, J. Chem. Phys. 73 (1980) 6021–6030.

[28] D. Massiot, F. Fayon, M. Capron, I. King, S.L. Calvé, B. Alonso, J.-O. Durand, e B. Bujoli, Z. Gan, G. Hoatson, Modelling one and two-dimensional solid-state NMR spectra, Magn. Reson. Chem. 40 (2002) 70–76.

[29] gosa-fit, website: http://bio-log.biz.

[30] T.D. Goddard, D.G. Kneller, Sparky 3, URL: http://www.cgl.ucsf.edu/home/sparky/, university of California, San Francisco (2007).

[31] M.R. Arnold, W. Kremer, H.-D. Lüdemann, H.R. Kalbitzer, ^{1}H-NMR parameters of common amino acid residues measured in aqueous solutions of the linear tetrapeptides Gly-Gly-X-Ala at pressures between 0.1 and 200 MPa, Biophys. Chemist. 96 (2002) 129–140.

[32] W. Rieping, M. Habeck, B. Bardiaux, A. Bernard, T.E. Malliavin, M. Nilges, ARIA2: automated NOE assignment and data integration in NMR structure calculation, Bioinformatics 23 (2007) 381–382.

[33] A.T. Brunger, Version 1.2 of the crystallography and NMR system, Nature Protocols 2 (2007) 2728–2733.

[34] R.A. Laskowski, J.A. Rullmann, M.W. MacArthur, R. Kaptein, J.M. Thornton, Aqua and procheck-nmr: programs for checking the quality of protein structures solved by NMR, J. Biomol. NMR 8 (1996) 477–486.

[35] N. Sreerama, R.W. Woody, Computation and analysis of protein circular dichroism spectra, Methods Enzymol. 383 (2004) 318–351.

[36] J.L. Markley, Correlation proton magnetic resonance studies at 250 MHz of bovine pancreatic ribonuclease. I. Reinvestigation of the histidine peak assignments, Biochemistry 14 (1975) 3546–3554.

[37] D. Wishart, B. Sykes, F. Richards, The chemical shift index: a fast and simple method for the assignment of protein secondary structure through NMR spectroscopy, Biochemistry 31 (1991) 1647–1651.

[38] R. Koradi, M. Billeter, K. Wüthrich, Molmol: a program for display and analysis of macromolecular structures, J. Mol. Graph. 14 (1996) 51–5, 29–32.

[39] W. Kabsch, C. Sander, Dictionary of protein secondary structure: pattern recognition of hydrogen-bonded and geometrical features, Biopolymers 22 (1983) 2577–2637.

[40] B.K. Ho, A. Thomas, R. Brasseur, Revisiting the Ramachandran plot: hard sphere repulsion, electrostatics, and H-bonding in the α-helix, Protein Science 12 (2003) 2508–2522.

[41] J.A. Killian, T.K.M. Nyholm, Peptides in lipid bilayers: the power of simple models, Curr. Opin. Struct. Biol. 16 (2006) 473–479.